*Advanced Powder Technol.*, Vol. 10, No. 1, pp. 1–20 (1999)


*Invited review*

# Brownian coagulation of submicron particles

ECKHARD OTTO and HEINZ FISSAN

*Process and Aerosol Measurement Technology, Gerhard-Mercator-University GH Duisburg, Bismarckstrasse 81, 47057 Duisburg, Germany*

Received 8 September 1998; accepted 28 September 1998

**Abstract**—Individual particles suspended in a fluid collide by various mechanisms such as random Brownian motion of particles, differential settling velocities, flow turbulence and by differential velocity gradients in laminar flow. Among these mechanisms, coagulation due to Brownian motion is an important particle growth mechanism in situations where small aerosol particles at a high concentration (as in flame reactors) or long-term behavior of suspended particles (as in the atmosphere) are concerned. In this paper the dynamical aerosol process — Brownian coagulation — is reviewed. The most often used formulas for describing the collision rate over the entire particle size regime are presented in a general form. Numerical modeling techniques used to describe the changes of the size distribution due to the coagulation process are described and discussed. Available analytical solutions are summarized.

*Keywords*: Brownian coagulation; modeling; lognormal; sectional; aerosol; analytical solution; self-preserving size distribution; modal.

## NOMENCLATURE

| | |
|---|---|
| $A_1, A_2, A_3$ | constants in slip correction |
| $\bar{c}$ | mean thermal velocity (cm/s) |
| $C$ | Cunningham slip correction factor (—) |
| $d$ | particle diameter (cm) |
| $d_{gn}$ | mean geometric particle diameter (cm) |
| $D$ | Diffusion coefficient ($cm^2/s$) |
| $f(Kn_P)$ | fitting function |
| $f_s$ | section spacing |
| $j$ | particle flux (collisions/s) |
| $J$ | particle flux (collisions/$cm^3$/s) |
| $k$ | counter for the $k$th moment |
| $k, i, j$ | number of section |

| | |
|---|---|
| $k_B$ | Boltzmann constant (g cm$^2$/s$^2$/K) |
| $K_{co}$ | collision coefficient for the continuum regime (cm$^3$/s) |
| $K_{fm}$ | collision coefficient for the free-molecule regime (cm$^{5/2}$/s) |
| Kn | Knudsen number (—) |
| $Kn_D$ | particle-Knudsen number defined by Dahneke (1983) (—) |
| $Kn_g$ | Knudsen number based on $r_g$ (—) |
| $M_k$ | $k$th moment of a log-normal size distribution (cm$^{3k}$/cm$^3$) |
| $N$ | total number concentration of particles (= $M_0$) (particles/cm$^3$) |
| $N_k$ | total number concentration of particles in each size class $k$ (particles/cm$^3$) |
| $N'$ | dimensionless number concentration $N/N_0$ (—) |
| $n$ | particle size distribution density function (particles/cm$^3$/cm$^3$) |
| $p$ | pressure (Pa) |
| $p_0$ | pressure at standard conditions ($1.013 \times 10^5$ Pa) |
| $q$ | positive integer, used to define the spacing factor |
| $r$ | particle radius (cm) |
| $r_g$ | geometric mean particle radius (cm) |
| $t$ | time (s) |
| $t'$ | dimensionless time (—) |
| $T$ | absolute temperature (K) |
| $T_0$ | reference temperature (23°C) |
| $T_S$ | Sutherland constant for air 110.4 K |
| $v$ | particle volume (cm$^3$) |
| $v_g$ | geometric mean particle volume (cm$^3$) |
| $Z$ | $\ln^2 \sigma$ (—) |

*Greek*

| | |
|---|---|
| $\beta$ | collision kernel (cm$^3$/s) |
| $\bar{\beta}$ | collision coefficient for a polydisperse aerosol (cm$^3$/s) |
| $\Delta$ | radius difference between the collision sphere and absorbing sphere (cm) |
| $\eta$ | particle volume in self-preserving coordinates (—) |
| $\lambda$ | mean free path of gas molecules (cm) |
| $\lambda_0$ | mean free path of gas molecules for air at standard conditions (67.3 nm) |
| $\lambda_P$ | mean free path of particles (cm) |
| $\mu$ | gas viscosity (g/cm/s) |

| | |
|---|---|
| $\mu_{23}$ | gas viscosity for air at standard conditions ($1.83245 \times 10^{-5}$ Pa s) |
| $\rho$ | particle density (g/cm$^3$) |
| $\sigma$ | geometric standard deviation based on particle radius (—) |
| $\Psi$ | particle size distribution in self-preserving coordinates (—) |

*Subscripts*

| | |
|---|---|
| 0 | refers to initial condition |
| $\infty$ | refers to condition at $t \rightarrow \infty$ |
| $\infty_{co}$ | refers to asymptotic condition within continuum regime |
| $\infty_{fm}$ | refers to asymptotic condition within free-molecule regime |
| co | refers to the continuum plus near-continuum regime |
| fm | refers to the free-molecule regime |

## 1. INTRODUCTION

An aerosol is a mixture of solid/liquid individual particles suspended in a gas. It is a dynamical system due to processes like diffusion, nucleation, condensation, coagulation, particle transport due to external forces, etc. In many situations only one of the above-mentioned processes is dominant. In many industrial processes coagulation is an important particle growth mechanism. Hereby individual particles collide by various mechanisms such as random Brownian motion. Brownian coagulation is dominant in situations where small aerosol particles at a high concentration are concerned (as in flame reactors) or long-term behavior of suspended particles (as in the atmosphere) is of interest. Coagulation of particles strongly influences the particle size distribution, and is therefore of fundamental interest in a wide range of applications in science, medicine and engineering. For that reason the rate of coagulation, i.e. the rate at which particles collide with each other, has been investigated by many researchers since von Smoluchowski's [1] basic work. For Brownian coagulation we have reviewed the most often used coagulation coefficients and give the table of Otto *et al.* [2]. They used a general form of the coagulation coefficient in which all the different coagulation rates fit.

## 2. COAGULATION COEFFICIENT

When particles collide and adhere to form a new, larger particle the process is called coagulation. The rate at which particles collide, the collision coefficient, can be calculated from Diffusion theory assuming that the particles are distributed homogeneously in the surrounding gas. To derive the collision rate we assume one particle fixed as a test particle and calculate the rate at which particles collide with this fixed particle by calculating the diffusion flux towards this fixed particle. We

describe the collision process for the assumption that the diffusion flux is described by the continuum diffusion theory. Since the movement of particles depends on the interaction between the particles and the surrounding gas, which is characterized by the Knudsen number, $\mathrm{Kn} = 2\lambda/d$, the resulting diffusion flux depends also on the Knudsen number. Consequently, collision coefficients in other Knudsen number regimes, e.g. the free-molecule regime, are based on other theories, e.g. kinetic theory of gases, but the flux can be determined in the same way. When the particles collide they stick together due to van der Waals forces. However, if the kinetic energy of the particles is too high particles can bounce off and the collision of particles does not result in coagulation. This can occur for particles smaller 10 nm due to their high thermal velocity and for particles larger 2 $\mu$m due to their greater mass. Therefore, the sticking probability of particles in the range between 10 nm and 2 $\mu$m is equal to one and the collision rate can be treated as the coagulation rate. Furthermore, we use the Smoluchowski [1] assumption of coalescence, i.e. the two colliding spherical particles form a new spherical particle conserving the mass.

The steady-state rate of collisions per second of particles (type 2) with a fixed particle (type 1) in the continuum regime is

$$j = 2\pi(d_1 + d_2) \cdot (D_1 + D_2)N_2. \tag{1}$$

'When there is more than one type 1 particle, the total collision rate between type 1 and type 2 particles per unit volume of fluid is the above derived collision rate multiplied by the concentration of type 1 particles, call it $N_1$' [3].

Thus the steady-state rate of collisions per unit volume per unit time between type 1 and type 2 particles is

$$J_{12} = 2\pi(d_1 + d_2) \cdot (D_1 + D_2)N_1N_2 = \beta_{12}N_1N_2. \tag{2}$$

The factor which makes the total flux of particles of type 2 towards particles of type 1, $J_{12}$, proportional to the number concentrations of type 1 and type 2 particles is the collision coefficient

$$\beta_{12} = 2\pi(d_1 + d_2) \cdot (D_1 + D_2). \tag{3}$$

$\beta_{12}$ ($\mathrm{cm}^3/\mathrm{s}$) is the Brownian coagulation coefficient for particles of diameter $d_1$ and $d_2$ in the continuum and near-continuum regime.

Figure 1 shows the steady state concentration profile of a diffusing particle 2 around a fixed particle 1 in different Knudsen number regimes. In the continuum regime the concentration profile of particles 2 follows the continuum theory, whereas the concentration in the free-molecule regime is unaffected of the presence of particle 1 and thus particles 2 just impact on the surface of particle 1 due to their normal motion. The concentration profile in the transition regime, however, has to be somewhere in the middle between these theories, as depicted in Fig. 1.

In the free-molecule regime, i.e. for particles having a Knudsen number, Kn, larger than about 50, here $\mathrm{Kn} = 2\lambda/d$ with $\lambda$ the mean free path of the surrounding gas and $d$ the particle diameter, the particles can be treated as molecules and the

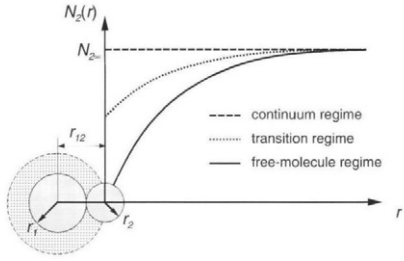


**Figure 1.** Steady-state concentration profiles of a diffusing particle 2 around a fixed particle 1.

collision rate can be calculated from the kinetic theory of gases. The collision kernel $\beta(v_1, v_2)$ is than given as

$$\beta(v_1, v_2) = \bar{c}_{12}\frac{\pi}{4}d_{12}^2 = \sqrt{\frac{8k_BT}{\pi m_1} + \frac{8k_BT}{\pi m_2}} \cdot \frac{\pi}{4}(d_1 + d_2)^2$$

$$= K_{fm}\left(v_1^{1/3} + v_2^{1/3}\right)^2\sqrt{\frac{1}{v_1} + \frac{1}{v_2}}, \tag{4}$$

where $\bar{c}_{12}$ is the mean thermal velocity of the particles, $K_{fm} = (3/4\pi)^{1/6} \times (6k_BT/\rho)^{1/2}$ is the coagulation constant for the free-molecule regime, $k_B$ is the Boltzmann constant, $T$ is the absolute temperature and $\rho$ is the particle density. Since we assumed here that the colliding particles have the same density $\rho$ it only appears in the coagulation constant $K_{fm}$.

In the continuum plus near-continuum regime, where the Knudsen number, Kn, is smaller than about 1, the particles behave like in a continuum and the diffusion theory for a continuum taking the slip correction into account can be used to obtain the collision coefficient

$$\beta(v_1, v_2) = 2\pi d_{12}D_{12} = K_{co}\left(v_1^{1/3} + v_2^{1/3}\right)\left(\frac{C_1}{v_1^{1/3}} + \frac{C_2}{v_2^{1/3}}\right), \tag{5}$$

where $K_{co} = 2k_BT/3\mu$ is the coagulation constant for the continuum plus near-continuum regime, $\mu$ is the gas viscosity and $C$ is the slip correction factor

$$C = 1 + \mathrm{Kn}\{A_1 + A_2\exp(-A_3/\mathrm{Kn})\}, \tag{6}$$

with the constants $A_1$, $A_2$ and $A_3$. Values of the constants are given in Allen and Raabe [4], whereas the values determined by Allen and Raabe [4] themselves are the most useful because they defined the viscosity as well as the mean free path with temperature- and pressure-dependent formulas in order to calculate the constants

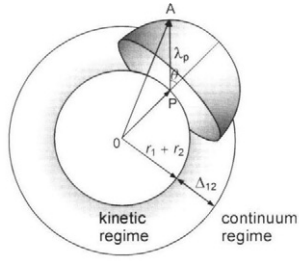


**Figure 2.** Absorbing sphere.

from their experiments. For the viscosity they used [5]:

$$\mu = \mu_{23}\left(\frac{T}{T_0}\right)^{1.5} \cdot \left(\frac{T_0 + T_S}{T + T_S}\right), \tag{7}$$

and for the mean free path of the gas [6]:

$$\lambda = \lambda_0\left(\frac{p_0}{p}\right) \cdot \left(\frac{T}{T_0}\right)^2 \cdot \left(\frac{T_0 + T_S}{T + T_S}\right), \tag{8}$$

where $\mu_{23} = 1.83245 \times 10^{-5}$ Pa s is the viscosity at 23°C, $T_S = 110.4$ K the Sutherland constant for air and $\lambda_0 = 67.3$ nm the mean free path of gas molecules in air at reference conditions $p_0 = 1.013 \times 10^5$ Pa and $T_0 = 296.15$ K.

The constants determined by Allen and Raabe [4] are:

$$A_1 = 1.142, \quad A_2 = 0.558, \quad A_3 = 0.999. \tag{9}$$

The entire transition regime is characterized by Knudsen numbers in the range of $\sim 1 < \mathrm{Kn} < \sim 50$. In the transition regime the coagulation rate is described neither by the continuum theory nor by simple kinetic theory. Fuchs [7] did find a semi-empirical solution of the coagulation coefficient by assuming that outside of a certain distance, i.e. an average mean free path of an aerosol particle, the transport of particles is described by the continuum diffusion theory including the slip-correction, and that inside the distance the particles behave like in a vacuum and the transport is described by simple kinetic theory. The two theories were brought together by matching the fluxes at the absorbing sphere radius. The absorbing sphere introduced by Fuchs is depicted in Fig. 2. Here $r_1 + r_2$ is the radius of the collision sphere, $\lambda_P$ the mean free path of the particles and $r_1 + r_2 + \Delta_{12}$ the radius of the absorbing sphere.

This so-called *flux matching* theory was the basis for most of the following theories because of its phenomenological approach and the guarantee that the collision function is valid over the entire size regime. All theories dealing with an absorbing sphere use a correction function first calculated by Fuchs. This function is mainly expressed as an enhancement of the collision function for the

**Table 1.**
Coefficients for the enhancement function $f(\mathrm{Kn_D})$

| Reference | $B_1$ | $B_2$ | $B_3$ |
|---|---|---|---|
| Fuchs [7] | $\frac{\Delta_{12}}{\lambda_D}$ | 2 | $2 \cdot \frac{\Delta_{12}}{\lambda_D}$ |
| Fuchs and Sutugin [9] | $\frac{3}{2}$ | $2 + 0.5655$ | 3 |
| Dahneke [8] | 1 | 2 | 2 |
| Harmonic mean | 0 | 2 | 0 |

near-continuum regime:

$$\beta = 2\pi D_{12} d_{12} \cdot f(\mathrm{Kn_P}), \tag{10}$$

with the diffusion coefficient $D_{12} = D_1 + D_2$ and the particle diameter $d_{12} = d_1 + d_2$ and $f(\mathrm{Kn_P})$ is a fitting function for the transition regime which depends on the particle Knudsen number. Several coagulation rates for the transition regime were discussed in Otto *et al.* [2]. They suggested to use Dahneke's [8] coagulation function because it reasonably well describes the Brownian coagulation process in the transition regime with minor numerical effort. In Dahneke's theory the particle mean free path is:

$$\lambda_P = \frac{2D_{12}}{\bar{c}_{12}}, \tag{11}$$

and the particle-Knudsen number:

$$\mathrm{Kn_D} = \frac{4D_{12}}{\bar{c}_{12} d_{12}}. \tag{12}$$

In the fitting function we use Dahneke's Knudsen number as well

$$f(\mathrm{Kn_D}) = \frac{1 + B_1 \mathrm{Kn_D}}{1 + B_2 \mathrm{Kn_D} + B_3 \mathrm{Kn_D^2}}. \tag{13}$$

The values for the coefficients $B_1$, $B_2$ and $B_3$ for some theories are listed in Table 1.

For Dahneke's theory [8] the enhancement function $f(\mathrm{Kn_D})$ is (Table 1)

$$f(\mathrm{Kn_D}) = \frac{1 + \mathrm{Kn_D}}{1 + 2\mathrm{Kn_D} + 2\mathrm{Kn_D^2}}. \tag{14}$$

Since the Knudsen number $\mathrm{Kn_D}$ is the ratio of the diffusion coefficient to the mean thermal velocity of the particles [equation (12)] it also can be written as the ratio of the coagulation coefficients of the limiting regimes [equations (4) and (5)]

$$\mathrm{Kn_D} = \frac{4D_{12}}{\bar{c}_{12} d_{12}} = \frac{1}{2} \cdot \frac{2\pi d_{12} D_{12}}{\frac{\pi}{4} \bar{c}_{12} d_{12}^2} = \frac{1}{2} \frac{\beta_{co}}{\beta_{fm}}. \tag{15}$$

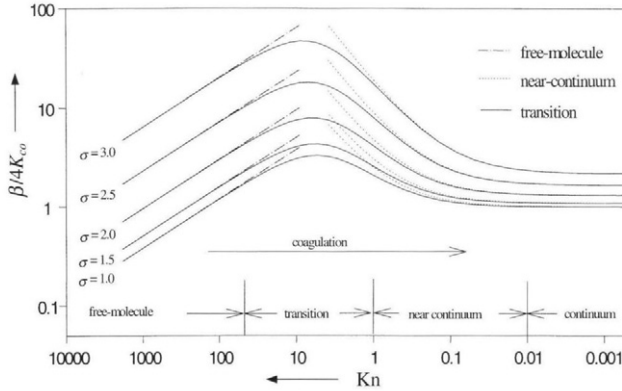


**Figure 3.** Coagulation coefficient as a function of Knudsen number using Dahnekes coefficient.

Since the particle-Knudsen number is the ratio of the coagulation coefficients of the limiting regimes, the coagulation coefficient for the transition regime can be expressed as a function of the limiting regimes. Dahneke's coagulation coefficient expressed as a function of the coagulation coefficients of the limiting regimes is [2]:

$$\beta = \beta_{\mathrm{co}} \frac{1 + \mathrm{Kn_D}}{1 + 2\mathrm{Kn_D} + 2\mathrm{Kn_D^2}}, \quad \text{with } \mathrm{Kn_D} = \frac{1}{2}\frac{\beta_{\mathrm{co}}}{\beta_{\mathrm{fm}}}. \tag{16}$$

Until now we considered that two particles meet each other. However, what is the difference when one of the particles is a molecule, i.e. we are talking about condensation? Or what if one of the particles is a charged ion, i.e. we are talking about particle charging? In principle nothing changes. In order to minimize the numerical effort the radius of the condensing species or the ion can be neglected. However, in these cases we have to discuss a sticking probability, which is sometimes called an accommodation or attachment coefficient, which must be multiplied with the free-molecule regime coagulation coefficient which is valid in the inner regime (Fig. 2).

Figure 3 shows the coagulation coefficient for the near-continuum regime, free-molecule regime and the transition regime for a log-normal distributed aerosol with specified geometric standard deviation. It can be seen that equation (16) smoothly combines the two limiting regimes.

## 3. MODELS

To understand the dynamical processes and to modify existing particle production lines, analytical and numerical models have been built over the last 30 years.

Von Smoluchowski [1] was the first to describe the change of the number concentration of a colloidal solution by assuming a constant collision coefficient.

Müller [10] extended the theory for polydispersed and bidispersed systems. The rate of change of the size distribution $n(v, t)$ of an aerosol by coagulation is

$$\frac{\partial n(v,t)}{\partial t} = \frac{1}{2}\int_0^v \beta(v-\bar{v},\bar{v})n(v-\bar{v},t)n(\bar{v},t)\,\mathrm{d}\bar{v} - n(v,t)\int_0^\infty \beta(v,\bar{v})n(\bar{v},t)\,\mathrm{d}\bar{v}, \tag{17}$$

where $\beta(v, \bar{v})$ specifies the collision rate between particles of volume $v$ and $\bar{v}$. The mechanisms resulting in particle collisions are treated in $\beta(v, \bar{v})$ as discussed above for Brownian coagulation.

Numerical methods must be applied in order to solve equation (17) for any aerosol. Some models developed assume a size distribution in order to obtain a solution. Only if the size distribution is known and fixed in shape can analytical solutions also be obtained.

### *3.1. Numerical solutions*

Different numerical approaches have been developed over the last years for solving equation (17). Figure 4 presents the modeling techniques most often used [11].

The easiest approach, assuming a monodisperse size distribution, works well for a first approximation, but no detailed information about the size distribution is gained. This technique needs one equation for each mode (two in the presented figure). A more complex modeling technique is the modal technique, where the size distribution is a superposition of multiple distinct distribution functions. If the log-normal function is used to describe a mode, three equations have to be solved for each mode (six for the example in Fig. 4). The sectional technique approximates the continuous size distribution by a finite number of sections, within each of which the size distribution function is assumed to be constant, i.e. the size distribution is a stepwise steady function. One equation in each section has to be solved either for the number concentration, volume concentration or volume square concentration [12, 13]. The accuracy of the sectional model depends on the number of sections used and on the numerically conserved integral property of the size distribution. In the spline technique the sections are smoothly jointed together by a polynomial fit (spline) [14, 15]. Using this technique an excellent reference model for the submicron size range can be developed; however, the disadvantage of this technique

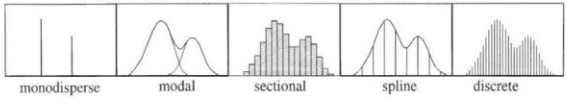


**Figure 4.** Most often used modeling techniques.

is the many equations that need to solve because in each section are at least three spline coefficients, i.e. three equations to solve. A technique which is correct only for very small clusters is the discrete technique. Here every discrete bin represents the number of primary particles. As one can imagine, the number of equations (each bin has to be solved) explodes for increasing coagulation time. Consequently, this technique is only useful for situations were particles are produced and coagulate just a bit, as in the early stages of particle production processes and for validation of other models. To use this detailed information in the very beginning but to reduce simulation time, many scientists combined the discrete technique (small particles) with one of the other techniques (coagulated particles) mentioned above [16].

Comparisons between sectional and spline models showed that the influence of neglecting the true shape of the size distribution and assuming a stepwise constant distribution is negligible when sections are very small. Thus, nowadays, the sectional technique can be treated as a reference technique in the submicron particle size range.

We will describe in more detail the sectional technique as a reference technique as well as the very time efficient modal technique in combination with the assumption of a log-normal size distribution.

*3.1.1. Discrete technique.* The discrete coagulation equation is given by:

$$\frac{\mathrm{d}N_k}{\mathrm{d}t} = \frac{1}{2}\sum_{j=1}^{k-1} \beta_{k-j,j} N_{k-j}(t) N_j(t) - N_k(t) \sum_{j=1}^{\infty} \beta_{k,j} N_j(t). \tag{18}$$

The left-hand side term gives the rate of change of the number concentration of size class $k$ by formation of particles of size class $k$ (first right-hand side term) and loss of particles of section $k$ by coagulation with all other particles (second right-hand side term). One equation must be solved for every existing $k$-mer. This makes this technique very accurate with regard to the size distribution, especially when particles will be formed with a constant size, so that really discrete sizes are present. However, this detailed information has to be paid for with an enormous computational effort. To reduce the computation time with minor loss of information, the discrete technique is often combined with the other mentioned techniques, i.e. having a discrete size distribution for the small particles (often about 20 discrete sizes) and starting then for the larger particles with a continuous size distribution formulation like the sectional technique.

*3.1.2. Sectional technique.* The main basic work in sectional modeling was done by Gelbard [12, 17, 18] and Wu and Flagan [19]. To reduce calculation time but allow a temperature change during coagulation, Landgrebe and Pratsinis [13] developed a sectional model using a dimensionless coagulation coefficient for the free-molecule regime.

In sectional formulation the particle size regime is sectionalized in the following way

$$f_s = \frac{v_{i+1}}{v_i}, \tag{19}$$

where $f_s$ is the section spacing, and $v_i$ and $v_{i+1}$ the section boundaries.

The sectional coagulation equation for the change of the number concentration is given by (e.g. [13]):

$$\frac{dN_k}{dt} = \frac{1}{2}\sum_{i=1}^{k-1}\sum_{j=1}^{k-1} {}^1\bar{\beta}_{i,j,k} N_i N_j - N_k \sum_{i=1}^{k-1} {}^2\bar{\beta}_{i,k} N_i + N_k \sum_{i=1}^{k-1} {}^5\bar{\beta}_{i,k} N_i$$
$$- \frac{1}{2}\,{}^3\bar{\beta}_k N_k^2 + \frac{1}{2}\,{}^6\bar{\beta}_k N_k^2 - N_k \sum_{i=k+1}^{m} {}^4\bar{\beta}_{i,k} N_i. \tag{20}$$

The left-hand side term gives the rate of change of the number concentration of section $k$. The first right-hand side term gives the formation of section $k$ particles from coagulations of two smaller particles. The second and third right-hand side terms account for the loss and gain of section $k$ particles, respectively, from coagulations of section $k$ particles with smaller ones. The fourth and fifth right-hand side terms account for the loss and gain, respectively, of section $k$ particles from coagulations between section $k$ particles themselves. The last right-hand side term gives the loss of section $k$ particles by coagulations between section $k$ particles and larger ones. The coagulation coefficients ${}^1\bar{\beta}$ to ${}^6\bar{\beta}$ are already integrated values which are given in detail as well in Landgrebe and Pratsinis [13]. They also investigated the influence of the balanced equation (number, volume or volume square). They stated '*the* $v^2$*-based model is seen to be most accurate, the volume-based model is second and the number-based model is least accurate*'.

Since Landgrebe and Pratsinis [13] developed a discrete-sectional model in terms of dimensionless variables, the model is very complex and is difficult to understand for people who are not familiar with sectional modeling. The main problem in understanding is the function $\Theta$ used to check whether the coagulation product belongs to the balanced section or not. Since these discontinuities have to be checked during integration, the solution technique is still wasteful concerning computation time. Lu [20] analyzed these discontinuities in the function $\Theta$ given by Landgrebe and Pratsinis [13] and removed them from the integrand by setting the integration limits in terms of relevant size parameters. As a consequence, the calculation of the integrals is easier to understand and the integral computation is much faster due to the discontinuity-free collision integrals. An approach based on the discrete formulation, i.e. no integration within each size interval, by using a representative particle volume instead of a section was developed by Hounslow *et al.* [21]. This model uses a section spacing factor $f_s = 2$. In order to make the model reliable to more exact solutions, which is frequently desirable, Litster *et al.* [22] ensured a smaller section spacing. In Landgrebe and Pratsinis [13] the section

spacing can be choosen freely, in Litster *et al.* [22] the section spacing must be

$$f_s = 2^{1/q}, \tag{21}$$

where $q$ is a positive integer. For $q = 1$ Litster *et al.* [22] reduces to Hounslow *et al.* [21]. It has to be mentioned that Litster wrote an Erratum to his paper which must be used for a small section spacing ($q > 4$). In the Erratum, however, equation (5) includes a misprint in sign in the fourth right-hand side term in the first exponential term. This can easily be checked by comparing the Litster *et al.* [22] equation (35) with the Erratum equation (5). This kind of section spacing [equation (21)] is also very useful when using the integration boundaries of Lu [20] because the number of integrals to be solved can be reduced.

Landgrebe and Pratsinis [13] stated that the smaller the section spacing, the more exact the results are because the influence of assuming a stepwise constant size distribution reduces more the smaller the section spacing is. Lu [20] stated the smaller the section spacing, the larger the relative error in each section, which seems to be in contradiction to Landgrebe and Pratsinis. However, Lu [20] did not state anything about the absolute error. As a result of these discussions we recommend to use a section spacing in the range of 1.2–1.5 which seems to produce good results in a gentle time. To obtain the best asymptotic results (self-preserving size distribution) we recommend a section spacing of smaller than 1.2 (Landgrebe and Pratsinis, [13] used 1.08). The asymptotic phenomenon of a coagulating aerosol is discussed in the section on self-preserving size distribution.

*3.1.3. Modal technique.* The modal technique is based on the assumption that a real aerosol can be represented by a superposition of several distinct size distributions which can be described by a mathematical function. The change of the size distribution is predicted by calculating the change of the moments (integral properties) of the size distribution. To close the set of moments a fixed mathematical function — very often the log-normal size distribution — has to be assumed. In aerosol physics the assumption of a log-normal size distribution is widely used because many real size distributions can be approximated very well by a log-normal function. Therefore, the log-normal approach was also used for coagulation, which implies that the functional form of the size distribution had to stay constant during coagulation.

The log-normal size distribution is given by

$$n(v,t) = \frac{N(t)}{3\sqrt{2\pi}\ln\sigma(t)} \exp\left[\frac{-\ln^2\{v/v_g(t)\}}{18\ln^2\sigma(t)}\right]\frac{1}{v}. \tag{22}$$

However, the log-normal size distribution offers some nice advantages. The first one is that the size distribution is known *a priori*, which reduces the integration procedure immensely. The second point is that the log-normal size distribution is described only by three parameters, i.e. the number concentration, $N(t)$, the mean geometric particle volume, $v_g(t)$, and the geometric standard deviation, $\sigma(t)$.

Instead of these three parameters three moments of the size distribution can be used. The moments of a size distribution are

$$M_k = \int_0^\infty v^k n(v,t)\,\mathrm{d}v. \tag{23}$$

Often used are $M_0$ as the total number concentration of particles, $N$, $M_1$ as the total volume concentration of particles, $V$, and $M_2$ as the volume square concentration, $V_2$, which for small particles is proportional to the scattered light.

The moment dynamic equation (MDE) for coagulation of a unimodal size distribution is given by:

$$\frac{\partial M_k}{\partial t} = \frac{1}{2}\int_0^\infty \int_0^\infty (v_1+v_2)^k \beta(v_1,v_2) n(v_1,t) n(v_2,t)\,\mathrm{d}v_1\,\mathrm{d}v_2 - \frac{1}{2}\int_0^\infty \int_0^\infty (v_1^k + v_2^k)\beta(v_1,v_2) n(v_1,t) n(v_2,t)\,\mathrm{d}v_1\,\mathrm{d}v_2. \tag{24}$$

The left-hand side term is the change of the $k$th moment of the size distribution, $M_k$, the first term on the right-hand side is the production of new particles and the second term the loss of particles due to coagulation. Three moments have to be solved for each mode assuming a log-normal size distribution for each mode. Thus for a multimodal size distribution a set of equations has to be set-up where additional terms account for the mass exchange between the modes. So in addition to the intramodal terms (inside one mode) given in equation (24) these equations show intermodal terms (between modes). Whitby *et al.* [11, 16] presented the equations for a bimodal size distribution.

The main numerical problem of equation (24) is the double integral. In order to solve these integrals numerically efficient the adapted Gauss–Hermite quadrature technique can be used [23]. However, they still need a lot of computation time, because the coagulation integrals have to be solved every time step with the modal technique. When using eight abscises the coagulation coefficient has to be calculated 64 times for each time step. When the integrals where centered [11] the number of calculations can be reduced to 32 by keeping the correctness. A much more elegant way is to express the double integrals again as a function of size distribution moments. The change of the size distribution can be calculated even faster applying this so-called method of moments. Together with the assumption of the log-normal size distribution, every moment can be expressed as function of the three parameters of the size distribution [24]. However, this technique is only practicable if the coagulation kernel is a homogeneous function. Otto *et al.* [2] presented a solution for the method of moments for the entire size regime based on Dahneke's coagulation coefficient and applying correction functions to equalize the inhomogeneities.

### *3.2. Analytical solutions*

The most elegant way of solving a mathematical problem is doing it by simple analytical analysis. However, analytical solutions are only possible in special cases for

most of the problems and also coagulation. Most of the analytical solutions imply an assumption of the size distribution function. Analytical solutions exist for the assumption of a monodisperse, a self-preserving and a log-normal size distribution.

*3.2.1. Monodisperse size distribution.* The easiest model is to assume that all the particles have the same size, i.e. the aerosol is monodisperse, and stays monodisperse during the coagulation process. This assumption reduces the size distribution to a single value. In addition the coagulation coefficient is assumed to be constant, which is valid in the continuum regime. In the other regimes a constant coagulation coefficient can just be assumed at the very beginning of the coagulation process. In these cases the number concentration decay is given by

$$N(t) = \frac{N_0}{1 + \frac{1}{2}\beta(v, \bar{v})N_0 t}, \tag{25}$$

and the change in the diameter, calculated from the conservation of mass during the coagulation process, is given by

$$d(t) = d_0 \cdot \left(1 + \frac{1}{2}\beta(v, \bar{v})N_0 t\right)^{1/3}. \tag{26}$$

This technique can be used to estimate the coagulation process in experiments or even to layout experiments. However, for detailed studies, information of the width of the size distribution, i.e. the standard deviation, which has an influence to the coagulation coefficient, is missing.

*3.2.2. Self-preserving size distribution.* Friedlander [25], Friedlander and Wang [26], Wang and Friedlander [27] and Lai *et al.* [28] developed a similarity theory for

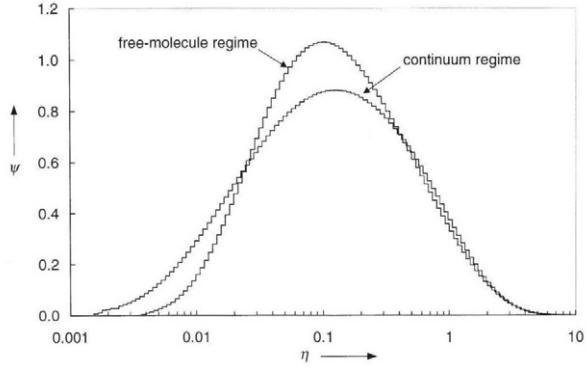


**Figure 5.** Self-preserving size distribution for the continuum regime as well as the free-molecule regime.

particle size distributions. They pointed out that after a sufficiently long coagulation time the size distribution did not change its shape, i.e. the standard deviation will not change and the size distribution is constant when transformed into the so-called self-preserving parameters.

$$\Psi(\eta) = \frac{n(v,t) \cdot V}{N(t)^2},$$
$$\eta = \frac{N(t) \cdot v}{V}. \tag{27}$$

Figure 5 shows the self-preserving size distribution for the continuum and the free-molecule regime calculated by Landgrebe and Pratsinis [13]. The stepwise shape comes from the sectional model used to calculate the shape of the self-preserving size distributions. Values of $\eta$ and $\Psi$ are tabulated for the free-molecule regime in Lai *et al.* [28] and in Graham and Robinson [29] more precisely (conserving the moments), and for the continuum regime in Friedlander and Wang [26]. The asymptotic geometric standard deviations in the continuum and free-molecule regime are $\sigma_g = 1.44$ [26] and $\sigma_g = 1.46$ [27], respectively. Since in the transition regime the coagulation coefficient is not a homogeneous function, the standard deviation changes with the mean geometric Knudsen number, $\mathrm{Kn}_g = 2\lambda/d_{gn}$ [27, 30]. The numerically derived quasi-self-preserving standard deviation for the transition regime using Fuchs' coagulation coefficient is depicted in Fig. 6 for a real aerosol, calculated with the sectional model of Landgrebe and Pratsinis [13], and a log-normal distributed aerosol [30]. Otto *et al.* [30] argued that the difference between the two models comes from the different shape of the size distribution. As the true self-preserving size distribution is not symmetrical, the appearing geometric standard deviation should be larger than of a symmetrically distribution as the log-normal size distribution. However, we saw for the log-normal size distribution that the obtained geometric standard deviation is also a function of the moments used to calculate the changes of the size distribution.

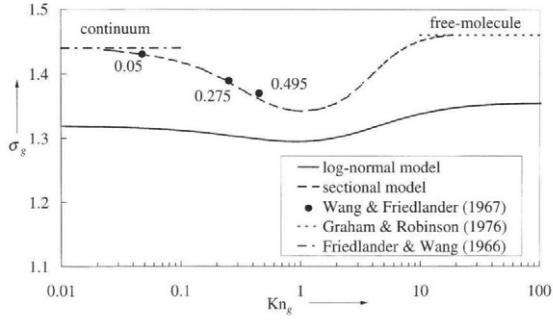


**Figure 6.** Quasi-self-preserving standard deviation for the sectional model and a log-normal model.

Applying the self-preserving size distribution theory to the free-molecule coagulation Lai *et al.* [28] derived:

$$N(t) = \frac{N_0}{\left[1 + \left(\frac{5}{3}\right)^2 K_{\mathrm{fm}} V^{1/6} N_0^{5/6} t\right]^{6/5}}. \tag{28}$$

This technique can be used in the free-molecular regime for size distributions which are close to the self-preserving size distribution.

*3.2.3. Log-normal size distribution.* The log-normal size distribution and the governing equation (MDE) was already described in Section 3.1.3. These are the equations to start with in order to obtain an analytical solution. For solving the change of the size distribution we use the moments of the size distribution

$$M_k = \int_0^\infty v^k n(v, t)\, \mathrm{d}v, \tag{29}$$

i.e. the total number concentration of particles, $M_0 = N$, the total volume concentration of particles, $M_1 = V$, and the volume square concentration, $M_2 = V_2$.

For the log-normal approach a self-preserving size distribution also exists, which is different to the one obtained by Friedlander and coworkers. Lee [24] and Lee *et al.* [31] calculated the log-normal size distribution in the continuum regime as well as in the free-molecule regime. For the transition regime Otto *et al.* [30] showed that only a quasi-self-preserving size distribution exists because here the standard deviation changes with Knudsen number. In addition analytical solutions have been obtained for the free-molecule regime [32] and for the continuum regime [24]. Recently, Park *et al.* [33] and Otto *et al.* [2] have developed an analytical solution for the entire size regime. The solution of Park *et al.* [33] is based on the harmonic mean of the coagulation coefficients of the near-continuum regime and the free-molecule regime, whereas the solution of Otto *et al.* [2] is based on Dahneke's coagulation coefficient. However, the differences in the results are minor, even if Park *et al.* uses the simpler and faster approach.

Here we repeat the solution of Park *et al.* [33] due to the simpler solution.

$$\begin{aligned} t' = {} & \frac{12s}{5}\left\{N'^{-5/6} - 1\right\} \\ & + \frac{3}{p}\left[\frac{1}{3}\left\{N'^{-1} - 1\right\} - \left(\frac{q}{2p}\right)\left\{N'^{-2/3} - 1\right\}\right. \\ & \left. + \left(\frac{q}{p}\right)^2\left\{N'^{-1/3} - 1\right\} - \left(\frac{q}{p}\right)^3 \ln\left\{\frac{p + q \cdot N'^{1/3}}{(p+q)\cdot N'^{1/3}}\right\}\right], \end{aligned} \tag{30}$$

$$Z = \ln^2 \sigma = \frac{1}{9}\ln\left[2x + N'\{\exp(9Z_0) - 2x\}\right], \tag{31}$$

$$\frac{v_g}{v_{g0}} = \frac{N'^{-1}\exp(9Z_0/2)}{\sqrt{2x + N'[\exp(9Z_0) - 2x]}}, \tag{32}$$

where

$t' = K_{co}N_0 t$

$N'(= N/N_0)$ is the dimensionless total particle number concentration

$p = 1 + \exp(Z_0)$

$q = 1.591 \cdot \mathrm{Kn}_0 \exp[1.5(Z_\infty - Z_0)] \cdot [\exp(Z_0/2) + \exp(5Z_0/2)]$

$Z_0 = \ln^2 \sigma_0$

$$H = \exp\left(\frac{25Z_0}{8}\right) + 2\exp\left(\frac{5Z_0}{8}\right) + \exp\left(\frac{Z_0}{8}\right)$$

$$s = \frac{K_{co}}{2b_0 K_{fm} H v_{go}^{1/6}}$$

$b_0 = 1 + 1.2\exp(-2\sigma_0) - 0.646\exp(-0.35\sigma_0^2)$

$$x = \frac{2s \cdot N'^{1/6} + \left[p + qN'^{1/3}\right]^{-1}}{2s \cdot N'^{1/6}\exp(-1.5 \cdot Z_{\infty,fm}) + \left[p + qN'^{1/3}\exp(-3Z_\infty)\right]^{-1}}$$

$Z_\infty = \ln^2 \sigma_\infty$

$Z_{\infty,fm} = \ln^2 \sigma_{\infty,fm}$

$\sigma_\infty(= 1.320)$ the asymptotic value of $\sigma$ for the continuum regime given by Lee [24].

$K_{co} = 2k_B T/3\mu$

$\mathrm{Kn}_0(= \lambda/r_{g0})$ the Knudsen number based on $r_{g0}$

$N_0$, $r_{g0}$, $v_{g0}$ and $\sigma_0$ are the initial values for $N$, $r_g$, $v_g$ and $\sigma$, respectively

0 and $\infty$ are referred to the initial condition and the $t \to \infty$ condition, respectively.

In Otto *et al.* [2] the two solutions are compared with numerical calculations in order to show the limits of the solution and the log-normal approach. They compared calculations with geometric standard deviations up to 1.8. The maximum relative error in the predicted number concentration was smaller than 20% after a dimensionless time of $t' = 10$, which is reasonably good for practical applications.

Otto *et al.* [2] provide a Microsoft® Excel file (E-mail: h.fissan@uni-duisburg.de or lee@kjist.ac.kr) including the solution of the papers Park *et al.* [33] and Otto *et al.* [2] at least 2 years after publication. This is a very good offer for scientists who are just interested in Brownian coagulation to compare with their own models and/or to check their measurements.

## 4. CONCLUSIONS

This paper presents several numerical methods as well as analytical solutions of the coagulation equation. Therefore, in a first step the most used coagulation coefficients are compared by fitting them into a universal enhancement function. Since Dahneke's coagulation function seems to be the best with minor numerical effort it is recommended for use over the entire size regime.

In a second step, possible numerical methods have been presented. Here we discussed that the discrete technique is often used to calculate the very beginning of coagulation but is too time consuming for larger coagulation times. In more detail we presented the two most promissing techniques for submicron particles, the sectional and the modal technique. In particular, the sectional technique can be treated as a reference technique due to the adjustable section spacing. In combination with the discrete technique for small particles (mono-, di-, tri-, . . .-mers) very detailed information of the size distribution can be obtained [13]. The presented modal aerosol dynamics modeling technique is much faster than the sectional technique and the moments of the size distribution just show minor differences. The big advantage of the modal technique is that it can easily account for additional aerosol dynamical processes like convection, diffusion, nucleation, condensation and the effect of external forces like thermophoresis or electrical forces [16, 34–36] without numerical diffusion. This makes it possible to implement this technique in computational fluid dynamics (CFD) codes and calculate two- or three-dimensional problems [2, 36, 37]. Applying sectional models to these problems is only possible when taking few sections and a large section spacing together with a super computer.

In a third step we presented several obtained analytical solutions, all based on the assumption of a size distribution. The solution providing most information with minor uncertainties is the analytical solution obtained by Park *et al.* [33]. They provide a Microsoft® Excel file via E-mail (h.fissan@uni-duisburg.de or lee@kjist.ac.kr) including already the whole analytical solution, which makes the coagulation problem easy to solve. The only handicap of the analytical solutions presented is that they can only be used for pure Brownian coagulation and cannot be extended for other effects.

## REFERENCES


1. M. von Smoluchowski, Versuch zur mathematischen Theorie der Koagulationskinetik kolloider Lösungen, *Z. Phys. Chem.* **92**, 129–168 (1918).
2. E. Otto, H. Fissan, S. H. Park and K. W. Lee, The log-normal size distribution theory of Brownian aerosol coagulation for the entire particle size range: part II: analytical solution using Dahnekes coagulation kernel, *J. Aerosol Sci.* **30**, 17–34 (1999).
3. J. H. Seinfeld, *Atmospheric Chemistry and Physics of Air Pollution*. Wiley, New York (1986).
4. M. D. Allen and O. G. Raabe, Slip correction measurements of spherical solid aerosol particles: in an improved Millikan apparatus, *Aerosol Sci. Technol.* **4**, 269–286 (1985).
5. H. Schlichting, *Boundary Layer Theory*. McGraw-Hill, New York (1968).
6. K. Willeke and P. A. Baron, *Aerosol Measurement*. Van Nostrand Reinhold, New York (1993).
7. N. A. Fuchs, *The Mechanics of Aerosols*. Pergamon Press, New York (1964).
8. B. Dahneke, Simple kinetic theory of Brownian diffusion in vapors and aerosols, in: *Theory of Dispersed Multiphase Flow*, R. E. Meyer (Ed.), pp. 97–133. Academic Press, New York (1983).
9. N. A. Fuchs and O. G. Sugutin, High-dispersed aerosols, in: *Topics in Current Aerosol Research*, G. M. Hidy and J. R. Brock (Eds), pp. 1–60. Pergamon Press, New York (1971).
10. H. Müller, Zur allgemeinen Theorie der raschen Koagulation, *Kolloidbeihefte* **27**, 223–250 (1928).
11. E. R. Whitby, P. H. McMurry, U. Shankar and F. S. Binkowski, Modal aerosol dynamics modeling, EPA Report for Contract No. 68-01-7365 (1991).
12. F. Gelbard, Y. Tambour and J. H. Seinfeld, Sectional representation for simulating aerosol dynamics, *J. Colloid Interface Sci.* **76**, 541–556 (1980).
13. J. D. Landgrebe and S. E. Pratsinis, A discrete-sectional model for powder production by gas phase chemical reaction and aerosol coagulation in the free-molecular regime, *J. Colloid Interface Sci.* **139**, 63–86 (1990).
14. F. Gelbard and J. H. Seinfeld, Numerical solutions of the dynamic equation for particle systems, *J. Comp. Phys.* **28**, 357–375 (1978).
15. K. P. Koutzenogii, A. I. Levykin and K. K. Sabelfeld, Kinetics of aerosol formation in the free molecule regime in presence of condensable vapor, *J. Aerosol Sci.* **27**, 665–679 (1996).
16. E. R. Whitby and P. H. McMurry, Modal aerosol dynamics modeling, *Aerosol Sci. Technol.* **27**, 673–688 (1997).
17. F. Gelbard and J. H. Seinfeld, Simulation of multicomponent aerosol dynamics, *J. Colloid Interface Sci.* **78**, 485–501 (1980).
18. F. Gelbard, Modeling multicomponent aerosol particle growth by vapor condensation, *Aerosol Sci. Technol.* **12**, 399–412 (1990).
19. J. J. Wu and R. C. Flagan, A discrete-sectional solution to the aerosol dynamics equation, *J. Colloid Interface Sci.* **123**, 339–352 (1988).
20. S. Y. Lu, Collision integrals of discrete-sectional model in simulating powder production, *AIChE J.* **40**, 1761–1764 (1994).
21. M. J. Hounslow, R. L. Ryall and V. R. Marshall, A discretized population balance for nucleation, growth and aggregation, *AIChE J.* **34**, 1821–1832 (1988).
22. J. D. Litster, D. J. Smit and M. J. Hounslow, Adjustable discretized population balance for growth and aggregation, *AIChE J.* **41**, 591–603 (1995).
23. W. H. Press, S. A. Teukolsky, W. T. Vetterling and B. P. Flannery, *Numerical Recipes in Fortran: The Art of Scientific Computing*. Cambridge University Press, New York (1992).
24. K. W. Lee, Change of particle size distribution during Brownian coagulation, *J. Colloid Interface Sci.* **92**, 315–325 (1983).
25. S. K. Friedlander, *Smoke, Dust and Haze*. Wiley, New York (1977).
26. S. K. Friedlander and C. S. Wang, The self-preserving particle size distribution for coagulation by Brownian motion, *J. Colloid Interface Sci.* **22**, 126–132 (1966).

27. C. S. Wang and S. K. Friedlander, The self-preserving particle size distribution for coagulation by Brownian motion, *J. Colloid Interface Sci.* **24**, 170–179 (1967).
28. F. S. Lai, S. K. Friedlander, J. Pich and G. M. Hidy, The self-preserving particle size distribution for Brownian coagulation in the free-molecule regime, *J. Colloid Interface Sci.* **39**, 395–405 (1972).
29. S. C. Graham and A. Robinson, A comparison of numerical solutions to the self-preserving size distribution for aerosol coagulation in the transition regime, *J. Aerosol Sci.* **7**, 261–273 (1976).
30. E. Otto, F. Stratmann, H. Fissan, S. Vemury and S. E. Pratsinis, Quasi-self-preserving log-normal size distribution in the transition regime, *Part. Part. Syst. Charact.* **11**, 359–366 (1994).
31. K. W. Lee, H. Chen and J. A. Gieseke, Log-normally preserving size distribution for Brownian coagulation in the free-molecule regime, *Aerosol Sci. Technol.* **3**, 53–62 (1984).
32. K. W. Lee, L. A. Curtis and H. Chen, An analytic solution to free-molecule aerosol coagulation, *Aerosol Sci. Technol.* **12**, 457–462 (1990).
33. S. H. Park, K. W. Lee, E. Otto and H. Fissan, The log-normal size distribution theory of Brownian aerosol coagulation for the entire particle size range: Part I: Analytical solution using the harmonic mean coagulation kernel, *J. Aerosol Sci.* **30**, 3–16 (1999).
34. S. E. Pratsinis, Simultaneous nucleation, condensation, and coagulation in aerosol reactors, *J. Colloid Interface Sci.* **124**, 416–427 (1988).
35. H. Bai and P. Biswas, Deposition of lognormally distributed aerosols accounting for simultaneous diffusion, thermophoresis and coagulation, *J. Aerosol Sci.* **21**, 629–640 (1990).
36. F. Stratmann, E. Otto and H. Fissan, Thermophoretical and diffusional particle transport in cooled laminar tube flow, *J. Aerosol Sci.* **25**, 1305–1319 (1994).
37. M. Wilck and F. Stratmann, A 2-D multicomponent modal aerosol model and its application to laminar flow reactors, *J. Aerosol Sci.* **28**, 959–972 (1997).